Probing the low-x structure of nuclear matter with diffractive hadron production in pA collisions

Yang Li[1] and Kirill Tuchin[1,2]
[1]*Department of Physics and Astronomy, Iowa State University, Ames, Iowa 50011, USA*
[2]*RIKEN BNL Research Center, Upton, New York 11973-5000, USA*
(Received 19 June 2008; published 19 August 2008)

We argue that hadron production in coherent diffraction of protons on a heavy nucleus provides a very sensitive probe of the low-x QCD dynamics. This process probes the BFKL dynamics in protons and the nonlinear gluon evolution in nuclei. We calculate the diffractive hadron production cross sections in the BNL Relativistic Heavy Ion Collider (RHIC) and CERN Large Hadron Collider (LHC) kinematic regions. To study the nuclear effects we introduce the diffractive nuclear modification factor. We show that, unlike the nuclear modification factor for inclusive hadron production that has very interesting dynamics at RHIC but is expected to be almost completely saturated at the LHC, the nuclear modification factor for diffractive production exhibits a nontrivial behavior at both RHIC and LHC.

DOI: 10.1103/PhysRevC.78.024905 PACS number(s): 24.85.+p, 13.75.−n, 25.75.−q

I. INTRODUCTION

Over the last decade we have witnessed a remarkable success of models based on gluon saturation in description of low-x data at HERA and BNL Relativistic Heavy Ion Collider (RHIC). This allowed quantification of several key features of the low-x dynamics of QCD. Still, there are many open questions such as the size of the next-to-leading order (NLO) corrections to the BK equation, the demarcation of the boundary between the kinematic regions of gluon saturation and the collinear factorization, etc. These problems can be addressed by probing the nuclear structure at even smaller x and/or by using a different set of measurements. In this article we argue that diffractive hadron production in pA collisions is a measurement that can provide a new handle on the low-x nuclear dynamics. Our study is motivated by the possibility of investigating the diffractive processes using the data on deuteron-gold (D-Au) collisions collected at RHIC.

A detailed theoretical analysis of coherent diffractive gluon production in onium–heavy nucleus ($q\bar{q}A$) collisions in the framework of the Color Glass Condensate [1–6] was performed in our previous publications [7,8]. There we argued that this process is sensitive to the low-x dynamics in both the onium and the nucleus. It has been argued in Refs. [9–11] that it is phenomenologically reasonable to approximate the proton light-cone wave function (away from fragmentation regions) by a system of color dipoles. Additionally, we demonstrate in Sec. II that the $qqqA$ propagator in the quasiclassical approximation takes exactly the same form as the $q\bar{q}A$ one if the emitted gluon transverse momentum is hard $k_T \gg Q_s$. In this approximation we can directly adopt the results of our theoretical analysis in Refs. [7] and [8]. The corresponding phenomenological approach is developed in Sec. III. A similar model has been used in Ref. [12] for the description of diffraction in pA collisions.

There are several parameters that govern the behavior of diffractive gluon production in pA collisions. These are gluon transverse momentum k_T and rapidity y, nucleus atomic number A, and transverse distance between the valence quarks r_T in a proton. The main observation of Refs. [7,8] is that the dependence of the diffractive hadron spectrum on these parameters in various kinematic regions is quite different. This provides a convenient handle on the behavior of the low-x gluon densities in the three most interesting kinematic regions: (i) the gluon saturation region $k_T < Q_s$, (ii) the geometric scaling region $k_T < Q_{\rm geom}$, and (iii) the hard perturbative QCD region $k_T > Q_{\rm geom}$.

The model that we use in this article is based on analysis of diffractive hadron production in all available kinematic regions. Equation (21) holds in the logarithmic approximation in all those regions and is therefore a convenient interpolation formula that we use to calculate the differential inclusive cross section (15). The transverse vector $\mathbf{I}(\mathbf{r}', \mathbf{k}, y)$ encodes information about the gluon density in the nucleus. It is related to an integral of the forward elastic gluon dipole scattering amplitude $N_A(\mathbf{r}', \mathbf{b}, y)$ over all intermediate dipole size [see Eqs. (16) and (17)]. This amplitude is parametrized according to the KKT model [13]. On the other hand, the dipole density $n(\mathbf{r}, \mathbf{r}', Y - y)$ encodes the gluon density in the proton, which is assumed to be dilute. Because the dipole density is a solution to the BFKL equation, we model it by the Leading Order (LO) BFKL amplitude in the diffusion approximation.

To compare the low-x dynamics in pA collisions to that in pp ones, it is convenient to introduce the *diffractive* nuclear modification factor $R^{pA}_{\rm diff}$ [see Eq. (31)]. We evaluate the diffractive gluon production in pp collisions as a limit $A \to 1$ of that in pA ones. Theoretical expectations for R^{pA} are detailed in Sec. III B and Sec. III C. The results of our numerical calculations performed using the KKT model [13] are presented in Sec. IV. We observe that $R^{pA}_{\rm diff}$ behavior is quite different from that of the nuclear modification factor $R^{pA}_{\rm incl}$ for inclusive hadron production. In the RHIC kinematic region, at moderately large k_T there is a significant enhancement of particle production in pA collisions [see Fig. 3]. This happens because the diffractive cross section at large k_T is proportional to the higher twist contribution that is enhanced in pA collisions by an additional factor of $A^{1/3}$. This enhancement gets increasingly compensated at forward rapidities by a suppression stemming from two sources:

(i) gluon saturation in the nucleus and (ii) shrinking of phase space available for the BFKL evolution in a proton [7]. The latter feature of the diffractive hadron production is apparent in Eq. (34) and is illustrated in Fig. 5, where we compare $R^{pA}_{\rm diff}$ for two different diffusion coefficients (switching the BFKL evolution on and off). In Fig. 4 and Fig. 6 we show $R^{pA}_{\rm diff}$ at CERN Large Hadron Collider (LHC). $R^{pA}_{\rm diff}$ exhibits rather strong dependence on rapidity. In contrast, $R^{pA}_{\rm incl}$ is not expected to change a lot at LHC [14]. This implies that by comparing inclusive and diffractive hadron production in the wide kinematic region of RHIC and LHC one will be able to infer much useful information about the higher twist contributions. Because different models of low-x dynamics predict different dependence of higher twists on atomic number A and energy/rapidity, measurements of diffractive hadron production will be instrumental in determining the valid physical mechanism for hadron production at high energies.

II. A MODEL FOR DIFFRACTIVE GLUON PRODUCTION IN pA COLLISIONS

A. Diffractive gluon production in $qqqA$ collisions

Coherent diffraction of a proton on a nucleus is a process, $p + A \to X + A$, characterized by a large rapidity gap between the diffractive system X and the *intact* nucleus A. A fraction of the coherent diffractive events increases with the collision energy and is expected to reach its limiting value of a half at asymptotically high energies. In the mean-field approximation $\alpha_s \ll 1$ and $A \gg 1$, the *incoherent* diffractive processes such as $p + A \to X + A^*$, where A^* is a diffractive system of color-neutral nuclear debris, are parametrically suppressed. Therefore, in the present article we consider only the coherent diffraction.[1] Coherent diffraction is possible only if the coherence length l_c of the emitted gluon with momentum k is larger than the nucleus size R_A (in the nucleus rest frame):

$$l_c = \frac{k_+}{\mathbf{k}^2} \gg R_A, \tag{1}$$

where $+$ indicates the light-cone direction of the incoming proton. The invariant mass of the produced system is given by $M^2 = \mathbf{k}^2/x$, where $x = k_+/p_+$ and p is the proton momentum. Substituting these equations in Eq. (1) yields the following condition on the mass of the diffractive system:

$$M^2 \ll \frac{p_+}{R_A} = \frac{s}{R_A m_p}, \tag{2}$$

where $\sqrt{s}$ is the center-of-mass energy of the proton–nucleon collision and m_p is proton mass.

A realistic model for diffractive gluon production in pA collisions was discussed by Kovchegov in Ref. [15]. He considered, in the quasiclassical approximation, emission of a gluon by a color-neutral qqq system of valence quarks with subsequent elastic interaction with a heavy nucleus. The resulting expressions for the propagators of the qqq and $qqqG$ systems in the nucleus can be written in the form [15]

$$\Pi_{ij} = v_i^T \left(e^{-M(\mathbf{z}_1)} - e^{-(2/9)(\chi_{12}+\chi_{13}+\chi_{23})}\right) \times \left(e^{-M(\mathbf{z}_2)} - e^{-(2/9)(\chi_{12}+\chi_{13}+\chi_{23})}\right) v_j, \tag{3}$$

where

$$v_1^T = \left(-1, -\frac{1}{\sqrt{3}}\right), \quad v_2^T = \left(1, -\frac{1}{\sqrt{3}}\right), \quad v_3^T = \left(0, \frac{2}{\sqrt{3}}\right), \tag{4}$$

the 2×2 matrix $M(\mathbf{z})$ is given by

$$M(\mathbf{z}) = \begin{pmatrix} \frac{1}{6}\zeta_3 + \frac{5}{12}(\zeta_2 + \zeta_1) + \frac{5}{36}(\chi_{23} + \chi_{13}) - \frac{1}{9}\chi_{12} & \frac{1}{4\sqrt{3}}(-\zeta_2 + \zeta_1 + \chi_{23} - \chi_{13}) \\ \frac{1}{4\sqrt{3}}(-\zeta_2 + \zeta_1 + \chi_{23} - \chi_{13}) & \frac{1}{2}\zeta_3 + \frac{1}{4}(\zeta_2 + \zeta_1) - \frac{1}{36}(\chi_{23} + \chi_{13}) + \frac{2}{9}\chi_{12} \end{pmatrix}, \tag{5}$$

and the scattering amplitudes of various dipoles on a nucleon read[2]

$$\zeta_i = \tfrac{1}{8}(\mathbf{z} - \mathbf{x}_i)^2 Q_{s0}^2 \qquad \chi_{ij} = \tfrac{1}{8}(\mathbf{x}_i - \mathbf{x}_j)^2 Q_{s0}^2, \tag{6}$$

where $\mathbf{x}_1, \mathbf{x}_2, \mathbf{x}_3$ are the valence quarks transverse coordinates and $\mathbf{z}_1$ and $\mathbf{z}_2$ are the gluon transverse coordinates in the amplitude and in the complex conjugated one, respectively (see Fig. 1).

The cross section for the diffractive gluon production in the quasiclassical approximation reads

$$\frac{d\sigma^{qqqA}}{d^2k_T dy} = \frac{\alpha_s}{(2\pi)^2\pi^2} \int d^2b d^2z_1 d^2z_2\, e^{-i\mathbf{k}\cdot(\mathbf{z}_1 - \mathbf{z}_2)} \times \sum_{i=1}^{3}\sum_{j=1}^{3} \frac{\mathbf{z}_1 - \mathbf{x}_i}{|\mathbf{z}_1 - \mathbf{x}_i|^2} \frac{\mathbf{z}_2 - \mathbf{x}_j}{|\mathbf{z}_2 - \mathbf{x}_j|^2} \Pi_{ij}. \tag{7}$$

Assume that the distances between the valence quarks are approximately the same: $\chi_{ij} \approx \chi = \frac{3}{4}R_p^2 Q_{s0}^2$, where R_p is the

[1] The incoherent diffraction may be phenomenologically important at RHIC and LHC energies [12,16].

[2] In this section only we adopted a shorthand notation where the saturation scale is understood to include the logarithmic dependence on the dipole size.

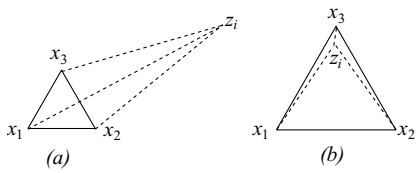

FIG. 1. Possible configurations formed by three valence quarks at positions $\mathbf{x}_1$, $\mathbf{x}_2$, and $\mathbf{x}_3$ and a gluon at position $\mathbf{z}_i$. We assumed that $x_{12} \approx x_{23} \approx x_{31}$. In (a) the sizes of the daughter dipoles are much bigger than the sizes of the parent dipoles. For small enough x_{12} this corresponds to the pQCD regime. In (b) one of the daughter dipoles is much smaller than the rest of the dipoles corresponding to the high density regime (see Ref. [17] for more details).

proton radius. Then, matrix M from Eq. (5) reduces to

$$M(\mathbf{z}) = \begin{pmatrix} \frac{1}{6}\zeta_3 + \frac{5}{12}(\zeta_2+\zeta_1) + \frac{1}{6}\chi & \frac{1}{4\sqrt{3}}(-\zeta_2+\zeta_1) \\ \frac{1}{4\sqrt{3}}(-\zeta_2+\zeta_1) & \frac{1}{2}\zeta_3 + \frac{1}{4}(\zeta_2+\zeta_1) + \frac{1}{6}\chi \end{pmatrix}. \tag{8}$$

In general, the propagators Π_{ij} are rather complicated objects. However, in the perturbative regime depicted in Fig. 1(a) they can be reduced to a simple sum of the corresponding $q\bar{q}G$ propagators as we are going to demonstrate now. The leading logarithmic contribution in the perturbative regime stems from the configuration shown in Fig. 1(a). In this case $\zeta_i \gg \chi$ and we have $\zeta_1 \approx \zeta_2 \approx \zeta_3 = \zeta$. Equation (8) becomes

$$M(\mathbf{z}) = \begin{pmatrix} \zeta & 0 \\ 0 & \zeta \end{pmatrix}. \tag{9}$$

Using Eqs. (3) and (4) we derive the propagator

$$\Pi_{ij} = \tfrac{4}{3}\left(e^{-\zeta(\mathbf{z}_1)} - e^{-\frac{2}{3}\chi}\right)\left(e^{-\zeta(\mathbf{z}_2)} - e^{-\frac{2}{3}\chi}\right)\left(\delta_{ij} - \tfrac{1}{2}(1-\delta_{ij})\right). \tag{10}$$

The cross section (7) reads in this case

$$\frac{d\sigma^{qqqA}}{d^2k_T dy} \approx \frac{\alpha_s}{(2\pi)^2\pi^2}\int d^2b d^2z_1 d^2z_2 e^{-i\mathbf{k}\cdot(\mathbf{z}_1-\mathbf{z}_2)} \times \frac{1}{2}\sum_{i<j}^{3}\left(\frac{\mathbf{z}_1-\mathbf{x}_i}{|\mathbf{z}_1-\mathbf{x}_i|^2} - \frac{\mathbf{z}_1-\mathbf{x}_j}{|\mathbf{z}_1-\mathbf{x}_j|^2}\right) \times \left(\frac{\mathbf{z}_2-\mathbf{x}_i}{|\mathbf{z}_2-\mathbf{x}_i|^2} - \frac{\mathbf{z}_2-\mathbf{x}_j}{|\mathbf{z}_2-\mathbf{x}_j|^2}\right)\Pi_{11}. \tag{11}$$

In the 't Hooft's limit, Eq. (11) can be related to the cross section for diffractive gluon production in quarkonium–nucleus collisions. To this end we introduce an effective color dipole with a quark and antiquark at points $\tilde{\mathbf{x}}_1$ and $\tilde{\mathbf{x}}_2$, respectively. Then, in the same approximation as in Fig. 1(a), we obtain

$$\frac{d\sigma^{q\bar{q}A}}{d^2k_T dy} \approx \frac{\alpha_s C_F}{\pi^2}\frac{1}{(2\pi)^2}\int d^2b d^2z_1 d^2z_2 \times \left(\frac{\mathbf{z}_1-\tilde{\mathbf{x}}_1}{|\mathbf{z}_1-\tilde{\mathbf{x}}_1|^2} - \frac{\mathbf{z}_1-\tilde{\mathbf{x}}_2}{|\mathbf{z}_1-\tilde{\mathbf{x}}_2|^2}\right) \times \left(\frac{\mathbf{z}_2-\tilde{\mathbf{x}}_1}{|\mathbf{z}_2-\tilde{\mathbf{x}}_1|^2} - \frac{\mathbf{z}_2-\tilde{\mathbf{x}}_2}{|\mathbf{z}_2-\tilde{\mathbf{x}}_2|^2}\right) \times e^{-i\mathbf{k}\cdot(\mathbf{z}_1-\mathbf{z}_2)}\left(e^{-\frac{1}{4}(\tilde{\mathbf{x}}_1-\mathbf{z}_1)^2\tilde{Q}_{s0}^2} - e^{-\frac{1}{8}(\tilde{\mathbf{x}}_1-\tilde{\mathbf{x}}_2)^2\tilde{Q}_{s0}^2}\right) \times \left(e^{-\frac{1}{4}(\tilde{\mathbf{x}}_1-\mathbf{z}_2)^2\tilde{Q}_{s0}^2} - e^{-\frac{1}{8}(\tilde{\mathbf{x}}_1-\tilde{\mathbf{x}}_2)^2\tilde{Q}_{s0}^2}\right). \tag{12}$$

Hence,

$$\frac{d\sigma^{qqqA}}{d^2k_T dy} \approx \frac{2}{C_F}\frac{d\sigma^{q\bar{q}A}}{d^2k_T dy} = \frac{3}{2}\frac{d\sigma^{q\bar{q}A}}{d^2k_T dy}. \tag{13}$$

Comparing arguments of exponents in Eq. (10) and in Eq. (12) we identify $\tilde{Q}_{s0}^2 = \frac{1}{2}Q_{s0}^2$ as an effective saturation scale and

$$\tilde{R}^2 \equiv (\tilde{\mathbf{x}}_1 - \tilde{\mathbf{x}}_2)^2 = 2\cdot\tfrac{2}{3}(\mathbf{x}_1-\mathbf{x}_2)^2 = \tfrac{4}{3}\cdot 3R_p^2 = (2R_p)^2 \tag{14}$$

as the square of the dipole size.[3] Expression (13) motivates a model that we adopt in this article. We assume that the pA cross section can be approximated by the $q\bar{q}A$ one with the dipole size given by Eq. (14). This model correctly reproduces the pQCD limit. It also satisfies the unitarity bound, which is achieved in the saturation regime depicted in Fig. 1(b).

B. Gluon production in quarkonium–heavy nucleus collisions

Now, as we set up a model for the diffractive gluon production in pA collisions in terms of the diffractive gluon production in $q\bar{q}A$ collisions, we review the main results that we derived for the latter case in our previous publications [7,8]. The cross section for the diffractive gluon production with transverse momentum k_T at rapidity y is given by

$$\frac{d\sigma^{pA}(k_T,y)}{d^2k_T dy} = \frac{\alpha_s C_F}{\pi^2}\frac{1}{(2\pi)^2}S_A \times \int d^2r' n_p(\mathbf{r},\mathbf{r}',Y-y)|\mathbf{I}(\mathbf{r}',\mathbf{k},y)|^2, \tag{15}$$

where $n_p(\mathbf{r},\mathbf{r}',Y-y)$ is the dipole density in the projectile proton. It has the meaning of the number of dipoles of size $\mathbf{r}'$ at rapidity $Y-y$ generated by evolution from the original dipole $\mathbf{r}$ having rapidity Y [18]. It satisfies the BFKL equation [19,20] with the initial condition (18). The two-dimensional vector function $\mathbf{I}(\mathbf{r}',\mathbf{k},y)$ is defined as

$$\mathbf{I}(\mathbf{r}',\mathbf{k},y) = -e^{-i\mathbf{k}\cdot\mathbf{r}'}i\nabla_{\mathbf{k}}Q(\mathbf{r}',\mathbf{k},y) + i\nabla_{\mathbf{k}}Q^*(\mathbf{r}',\mathbf{k},y), \tag{16}$$

where

$$Q(\mathbf{r}',\mathbf{k},y) = -\int d^2w e^{i\mathbf{k}\cdot\mathbf{w}}\frac{1}{w^2}\times[N_A(\mathbf{r}',\mathbf{b},y) - N_A \times (\mathbf{w}-\mathbf{r}',\mathbf{b},y) - N_A(\mathbf{w},\mathbf{b},y) + N_A(\mathbf{w}-\mathbf{r}',\mathbf{b},y)N_A(\mathbf{w},\mathbf{b},y)]. \tag{17}$$

The vector function $\mathbf{I}(\mathbf{r}',\mathbf{k},y)$ incorporates information about two physical processes: (i) gluon emission off the daughter dipole $\mathbf{r}'$ produced in the course of the BFKL evolution and (ii) low-x gluon evolution in the nucleus through $N_A(\mathbf{r},\mathbf{b},y)$, which is the dipole-nucleus forward elastic scattering amplitude satisfying the BK equation [21,22]. In the quasiclassical approximation the dipole density reads

$$n_p(\mathbf{r},\mathbf{r}',0) = \delta(\mathbf{r}-\mathbf{r}'), \tag{18}$$

[3] In the following we are going to discuss only onium–nucleus scattering. Therefore we will omit the tildes to simplify notations.

while the scattering amplitude is given by the Glauber-Mueller formula [23] (now we explicitly write down the logarithm in the exponent)

$$N_A(\mathbf{r},\mathbf{b},0) = 1 - e^{-\frac{1}{8}\mathbf{r}^2 Q_{s0}^2 \ln\frac{1}{r\Lambda}}, \tag{19}$$

where Q_{s0} is the saturation scale at rapidity $y = 0$. In the case of dipole–proton scattering we expand Eq. (19) and get

$$N_p(\mathbf{r},\mathbf{b},0) = \frac{1}{8}\mathbf{r}^2\,\Lambda^2 \ln\frac{1}{r\Lambda}. \tag{20}$$

In all limiting cases we can write [8]

$$|\mathbf{I}(\mathbf{r}',\mathbf{k},y)|^2 \approx C\,\frac{4\,(2\pi)^2}{k^2} N_A^2(k^{-1}\hat{\mathbf{k}},\mathbf{b},y) \times [1 - N_A(\mathbf{r}',\mathbf{b},y)]^2\,\sin^2\left(\frac{\mathbf{k}\cdot\mathbf{r}'}{2}\right), \tag{21}$$

where C is a constant of order unity (its precise value, which can be found in Ref. [8], is of little importance here). Let us emphasize, that Eq. (21) holds *asymptotically* in *all* kinematic regions. Due to the initial condition (18), the cross section in the quasiclassical approximation is merely proportional to $|\mathbf{I}(\mathbf{r}',\mathbf{k},y)|^2$. Accordingly, employing Eq. (21) we obtain

$$\frac{d\sigma^{pA}(R,k_T,0)}{d^2k_T dy} \approx C\,\frac{4\,\alpha_s C_F}{\pi^2}\,\frac{S_A}{k_T^2} N_A^2\left(k_T^{-1},\mathbf{b},0\right) \times [1 - N_A(R,\mathbf{b},0)]^2\,\sin^2\left(\frac{\mathbf{k}\cdot\mathbf{R}}{2}\right). \tag{22}$$

At larger rapidities we integrate over $\mathbf{r}'$ in Eq. (15) using Eq. (21). In the case of hard gluons we get

$$\frac{d\sigma^{pA}(R,k_T,y)}{d^2k_T dy} = \frac{\alpha_s C_F}{\pi^{5/2}} S_A\, N_A^2(k^{-1},\mathbf{b},y) \times \frac{\min\left\{\frac{1}{k_T^2}, R^2\right\}}{(2\bar{\alpha}_s(Y-y)|\ln(Rk_T)|)^{1/4}} \times e^{2\sqrt{2\bar{\alpha}_s(Y-y)|\ln(Rk_T)|}}, \quad k_T > Q_s, \tag{23}$$

where $\bar{\alpha}_s = \alpha_s N_c/\pi$. The cross section for the soft gluon production by a large dipole reads

$$\frac{d\sigma^{pA}(R,k_T,y)}{d^2k_T dy} = \frac{\alpha_s C_F}{8\pi^{5/2}}\,\frac{S_A}{Q_s^2}\,\frac{(2\bar{\alpha}_s(Y-y))^{1/4}}{\ln^{3/4}(RQ_s)} \times e^{2\sqrt{2\bar{\alpha}_s(Y-y)\ln(RQ_s)}}, \quad R, \quad \frac{1}{k_T} > \frac{1}{Q_s}, \tag{24}$$

while in the case of soft gluon emission by a small onium

$$\frac{d\sigma^{pA}(R,k_T,y)}{d^2k_T dy} = \frac{\alpha_s C_F}{4\pi^{5/2}}\,S_A R^2\,\frac{1}{\left(2\bar{\alpha}_s(Y-y)\ln\frac{1}{RQ_s}\right)^{1/4}} \times e^{2\sqrt{2\bar{\alpha}_s(Y-y)\ln\frac{1}{RQ_s}}}, \quad R < \frac{1}{Q_s} < \frac{1}{k_T}. \tag{25}$$

In all the reviewed cases, Eqs. (23)–(25), gluon multiplicity arises from the cut Pomeron that is hooked up to the incoming proton.

C. Forward dipole–nucleus scattering amplitude

The last required ingredient is the forward elastic scattering amplitude $N_A(\mathbf{r},\mathbf{b},y)$. It can be evaluated in various kinematic regions. In the double logarithmic approximation (DLA)

$$N_A(\mathbf{r},\mathbf{b},y) = \frac{\sqrt{\pi}}{16\pi}\,\frac{\ln^{1/4}\left(\frac{1}{rQ_{s0}}\right)}{(2\bar{\alpha}_s y)^{3/4}}\,r^2 Q_{s0}^2 \times \left(1 + \sqrt{\frac{2\bar{\alpha}_s y}{\ln\frac{1}{rQ_{s0}}}}\ln\frac{Q_{s0}}{\Lambda}\right) e^{2\sqrt{2\bar{\alpha}_s y\ln\frac{1}{rQ_{s0}}}}, \quad r < 1/Q_{s0}, \quad \ln\frac{1}{rQ_{s0}} \gg \alpha_s y. \tag{26}$$

This limit coincides with the small x and small r limit of the DGLAP equation. It obviously breaks the geometric scaling. Consequently, the DLA holds in the transition region between the gluon saturation and the hard perturbative QCD characterized by a hard scale k_H, i.e., when $Q_{\rm geom} < k_T < k_H$, where $Q_{\rm geom}$ is the scale at which the geometric scaling breaks down. It reads in the DLA

$$Q_{\rm geom} \approx \frac{Q_s^2}{Q_{s0}}. \tag{27}$$

The saturation scale is given by

$$Q_s \approx A^{1/3}\Lambda^2 e^{\lambda Y}, \tag{28}$$

where $\lambda \approx 2\bar{\alpha}_s$ in the DLA. The hard scale k_H can be related to the invariant mass of the diffractively produced system as discussed in Sec. II A in detail.

As we approach the saturation region by decreasing k_T at fixed rapidity we arrive at the diffusion approximation

$$N_A(\mathbf{r},\mathbf{b},y) = \frac{rQ_{s0}}{8\pi}\sqrt{\frac{\pi}{14\zeta(3)\bar{\alpha}_s y}}\ln\left(\frac{Q_{s0}}{\Lambda}\right) e^{(\alpha_P-1)y} e^{-\frac{\ln^2(rQ_{s0})}{14\zeta(3)\bar{\alpha}_s y}}, \quad \alpha_s y \gg \ln^2\left(\frac{1}{rQ_{s0}}\right), \tag{29}$$

where the BFKL Pomeron intercept is $\alpha_P - 1 = 4\bar{\alpha}_s \ln 2$. We observe that the amplitude geometrically scales modulo small diffusive corrections. The diffusion approximation (29) holds in the kinematic region $Q_s < k_T < Q_{\rm geom}$.

Finally, deeply in the saturation region where $k_T < Q_s$, the solution to the BK equation reads [17]

$$N_A(\mathbf{r},\mathbf{b},y) = 1 - S_0 e^{-\tau^2/8} = 1 - S_0 e^{-\frac{1}{8}\ln^2(r^2Q_s^2)}, \quad r \gg \frac{1}{Q_s}. \tag{30}$$

III. NUCLEAR EFFECTS IN DIFFRACTIVE GLUON PRODUCTION

A. Nuclear modification factor

A convenient way to study the nuclear dependence of particle production is to consider the nuclear modification factor defined as

$$R_{\rm diff}^{pA}(k_T,\,y)=\frac{\frac{d\sigma_{\rm diff}^{pA}(k_T,y)}{d^2k_T dy}}{A\,\frac{d\sigma_{\rm diff}^{pp}(k_T,y)}{d^2k_T dy}}. \tag{31}$$

If the production process is completely incoherent then $R_{\rm diff}^{pA}(k_T,\,y)=1$. In the case of inclusive gluon production, the nuclear modification factor $R_{\rm incl}^{pA}$ was discussed in detail in Ref. [24]. It has been demonstrated that in the extended geometric scaling region $Q_s(y)\lesssim k_T\lesssim Q_{\rm geom}$, the nuclear modification factor is suppressed as $R_{\rm incl}^{pA}\sim A^{-1/6}$, while in the saturation region $k_T\lesssim Q_s(y)$ the suppression is $R_{\rm incl}^{pA}\sim A^{-1/3}$. The amount of suppression is closely related to the value of the anomalous dimension γ in a given kinematic region. At rapidity $y\simeq 0$ at RHIC $R_{\rm incl}^{pA}$ exhibits slight enhancement (Cronin effect), which serves as an indicator that the low-x evolution in that process does not play an important role. We argue below that the behavior of $R_{\rm diff}^{pA}$ is quite different from that of the inclusive one which makes it a convenient tool for the study of low-x gluon dynamics.

In the previous section we addressed in detail the diffractive gluon production in pA collisions. To evaluate the $R_{\rm diff}^{pA}$ we need to normalize it by that in pp collisions. The latter is obtained by replacing the forward elastic dipole–nucleus scattering amplitude given by Eq. (26) with the corresponding forward elastic dipole–proton scattering amplitude

$$N_p(\mathbf{r},\,\mathbf{b},\,y)=\frac{\sqrt{\pi}}{16\pi}\,\frac{\ln^{1/4}\left(\frac{1}{r\Lambda}\right)}{(2\bar\alpha_s y)^{3/4}}\,r^2\Lambda^2 e^{2\sqrt{2\bar\alpha_s y\ln\frac{1}{r\Lambda}}}. \tag{32}$$

In Eq. (26) we replaced Q_{s0} by Λ and set $A=1$. Because we assume that the gluon saturation effects are negligible in the proton, the cross section for the diffractive gluon production in pp collisions in the case of large characteristic proton size is obtained from Eq. (23) by setting $A=1$ with the result

$$\begin{aligned}\frac{d\sigma^{pp}(R,k_T,y)}{d^2k_T dy}&=\frac{\alpha_s C_F}{\pi^{5/2}}\min\left\{\frac{1}{k_T^2},\,R^2\right\}S_p\,N_p^2\left(k_T^{-1}\hat{\mathbf{k}},\,\mathbf{b},\,y\right)\\&\times\frac{1}{(2\bar\alpha_s(Y-y)|\ln(Rk_T)|)^{1/4}}\\&\times e^{2\sqrt{2\bar\alpha_s(Y-y)|\ln(Rk_T)|}}.\end{aligned} \tag{33}$$

Similarly, we get in the quasiclassical approximation using Eq. (22)

$$\begin{aligned}\frac{d\sigma^{pp}(R,k_T,0)}{d^2k_T dy}&\approx C\,\frac{4\alpha_s C_F}{\pi^2}\,\frac{S_p}{k_T^2}\,\frac{\Lambda^4}{64\,k_T^4}\,\ln^2\left(\frac{k_T}{\Lambda}\right)\\&\times e^{-\frac{1}{4}R^2\Lambda^2}\,\frac{1}{2}(1-J_0(Rk_T)),\end{aligned} \tag{34}$$

where we averaged over the directions of the dipole $\mathbf{R}$ according to

$$\frac{1}{\pi}\int_0^\pi d\theta\,\sin^2\left(\frac{1}{2}k_T R\cos\theta\right)=\frac{1}{2}(1-J_0(Rk_T)). \tag{35}$$

Gluon saturation effects in protons may be important at backward rapidities at LHC. Taking them into account constitutes a difficult and not yet solved problem. Fortunately, effects associated with the gluon saturation in protons are not expected to significantly alter the nuclear dependence of our results because they are likely to cancel between the numerator and denominator of Eq. (31).

B. Quasiclassical approximation

The nuclear modification factor in the quasiclassical approximation and at high transverse momenta is derived by substitution of Eqs. (22) and (34) into Eq. (31) and deducing

$$\begin{aligned}R_{\rm diff}^{pA}(k_T,0)&=A^{1/3}\left(1-\frac{1}{8}A^{1/3}\frac{\Lambda^2}{2\,k_T^2}\ln\frac{k_T}{\Lambda}\right)\\&\times e^{-\frac{1}{4}R^2Q_{s0}^2},\quad k_T\gg Q_{s0},\end{aligned} \tag{36}$$

where we take into account that $S_A=A^{2/3}S_p$ and $Q_{s0}^2=A^{1/3}\Lambda^2$. According to Eq. (36) at very large k_T and fixed A the nuclear modification factor approaches a constant,

$$R_{\rm diff}^{pA}(k_T,0)\to A^{1/3}e^{-\frac{1}{4}A^{1/3}\ln A^{1/3}},\quad k_T\to\infty. \tag{37}$$

Equation (36) implies that $R_{\rm diff}^{pA}(k_T,0)$ approaches unity from below as $k_T\to\infty$. In contrast to $R_{\rm diff}^{pA}(k_T,0)$, the nuclear modification factor for inclusive gluon production receives a positive power correction that is a source of the Cronin enhancement observed in inclusive gluon production in pA collisions.

In the saturation region we derive

$$R_{\rm diff}^{pA}(k_T,0)=\frac{64k_T^4}{A^{1/3}\Lambda^4\ln^2\frac{1}{R\Lambda}}\,e^{-\frac{1}{4}R^2Q_{s0}^2},\quad k_T\ll Q_{s0}. \tag{38}$$

That is, the nuclear modification factor vanishes at small momenta as k_T^4. Actually, if we neglect the slow logarithmic dependence of the initial saturation scale Q_{s0} on r in Eq. (19), the integral appearing in Eq. (17) can be taken analytically. The corresponding result can be found in Ref. [15]. In Fig. 2 we use this analytical result to plot the nuclear modification factor $R_{\rm diff}^{pA}$ as a function of transverse momentum k_T.

We observe that, unlike in the inclusive gluon production case, the size of the incoming projectile plays a very important role in the diffractive production. What is important is the relationship between the quarkonium size R and the inverse saturation scale $1/Q_s$. In the quasiclassical approximation, that is, neglecting the low-x evolution, the diffractive gluon production is exponentially suppressed for heavy nuclei if $R>1/Q_s$ as compared to light nuclei. If $R<1/Q_s$, suppression gives way to enhancement at high transverse momenta. Both effects come about as the result of the coherent scattering of protons off nucleus.

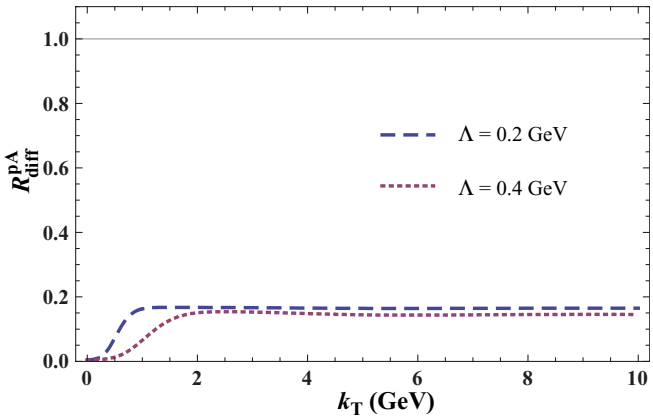

FIG. 2. (Color online) Nuclear modification factor $R_{\rm diff}^{pA}$ as a function of transverse momentum k_T in the quasiclassical approximation. Λ is a nonperturbative momentum scale.

C. Low-x evolution: Hard gluons

1. Double logarithmic approximation

The low-x evolution has a dramatic effect on the diffractive gluon production. We would like to start our analyses with the case of moderately large transverse momentum such that the geometric scaling is broken, but the interaction is still coherent. Substituting Eqs. (23) and (33) into Eq. (31) we derive that, in general,

$$R_{\rm diff}^{pA}(R, k_T, y) = \frac{1}{A^{1/3}} \frac{N_A^2\left(k_T^{-1}, \mathbf{b}, y\right)}{N_p^2\left(k_T^{-1}, \mathbf{b}, y\right)}, \quad k_T \gg Q_s. \tag{39}$$

In the double logarithmic approximation, the BFKL equation coincides with the DGLAP equation. Therefore, in this region we can observe crossover from the coherent small-x dynamics to incoherent hard perturbative QCD. Using Eqs. (26) and (32) in Eq. (39) we derive

$$R_{\rm diff}^{pA}(k_T, y) = \frac{S_A}{AS_p} \sqrt{\frac{\ln\frac{k_T}{Q_{s0}}}{\ln\frac{k_T}{\Lambda}}} \frac{Q_{s0}^4}{\Lambda^4} \left(1 + \sqrt{\frac{2\bar{\alpha}_s y}{\ln\frac{k_T}{Q_{s0}}}} \ln\frac{Q_{s0}}{\Lambda}\right)^2 \times e^{4\sqrt{2\bar{\alpha}_s y}\left(\sqrt{\ln\frac{k_T}{Q_{s0}}} - \sqrt{\ln\frac{k_T}{\Lambda}}\right)}, \quad k_T \gg Q_{\rm geom}. \tag{40}$$

Introducing a new variable [24]

$$\zeta = \left(\frac{\ln\frac{k_T}{Q_{s0}}}{\ln\frac{k_T}{\Lambda}}\right)^{1/4}, \tag{41}$$

we reduce Eq. (40) to

$$R_{\rm diff}^{pA}(k_T, y) = A^{1/3}\zeta^2 \left(1 + \sqrt{2\bar{\alpha}_s y \ln\frac{Q_{s0}}{\Lambda}} \frac{\sqrt{1-\zeta^4}}{\zeta^2}\right)^2 \times \exp\left\{-4\sqrt{2\bar{\alpha}_s y \ln\frac{Q_{s0}}{\Lambda}} \sqrt{\frac{1-\zeta^2}{1+\zeta^2}}\right\}. \tag{42}$$

The DLA approximation is valid when $k_T \gg Q_s(y) > Q_{s0}$. In this case Eq. (42) becomes

$$R_{\rm diff}^{pA}(k_T, y) \approx A^{1/3}\left(1 - \sqrt{2\bar{\alpha}_s y} \frac{\ln\frac{Q_{s0}}{\Lambda}}{\sqrt{\ln\frac{k_T}{\Lambda}}}\right), \quad k_T \gg Q_{\rm geom}. \tag{43}$$

The remarkable feature of this result is enhancement of the nuclear modification factor by $A^{1/3}$. Unlike the quasiclassical case, Eq. (37), this enhancement is not overrun at large A by a small exponential factor. The reason is that in the course of low-x BFKL evolution dipoles with small size $r < 1/Q_s$ are produced and these dominate the cross section. Let us also mention that an enhancement similar to Eq. (43) has already been discussed in the context of the J/ψ production off the nuclear targets [25] as well as in the breakdown of the collinear factorization of the fragmentation functions [26].

It is important to emphasize that the result (43) holds only as long as the coherence length $l_c \approx \frac{1}{2M_N x}$ is much larger than the nuclear size. Because in the center-of-mass frame kinematics $x = \frac{k_T}{\sqrt{s}} e^{-y}$, at large enough transverse momentum k_T and fixed rapidity y and energy s the coherence is lost and the nuclear modification factor approaches unity. Therefore, the region where $R_{\rm diff}^{pA} \sim A^{1/3}$ scaling gives way to $R_{\rm diff}^{pA} \sim 1$ is the transition region between the semihard nuclear fields and the hard perturbative QCD. Needless to say that identification of this region is crucial for understanding the interplay between the dense and dilute high energy QCD regimes.

2. Extended geometric scaling region

Next, we analyze the extended geometric scaling region $Q_s(y) < k_T < Q_{\rm geom}$. Here the evolution is still linear and is well approximated by the leading twist approximation. However, the anomalous dimension of the gluon distribution significantly departs from unity and approaches the value it has at the critical line $k_T = Q_s(y)$. It is therefore appropriate to use the leading logarithmic approximation for the function $N_A(\mathbf{r}, \mathbf{b}, y)$. Substituting Eqs. (29) and (32) in Eq. (39), we derive

$$R_{\rm diff}^{pA}(k_T, y) = \frac{4}{7\zeta(3)} \frac{k_T^2}{\Lambda^2} \frac{\ln^2\left(\frac{Q_{s0}}{\Lambda}\right)\sqrt{2\bar{\alpha}_s y}}{\sqrt{\ln\frac{k_T}{\Lambda}}} \exp\left\{2(\alpha_P - 1)y - 4\sqrt{2\bar{\alpha}_s y \ln\frac{k_T}{\Lambda}} - \frac{2\ln^2\left(\frac{Q_{s0}}{k_T}\right)}{14\zeta(3)\bar{\alpha}_s y}\right\}, \quad Q_s < k_T < Q_{\rm geom}. \tag{44}$$

This equation clearly demonstrates that the A dependence of the nuclear modification factor arises only through the slow-varying logarithmic factors. As far as the rapidity dependence is concerned, we can estimate it at the scale $k_T = Q_{\rm geom}(y)$. Because $N_A(\mathbf{r}, \mathbf{b}, y)$ is constant on the critical line, we derive

$$R_{\rm diff}^{pA}(Q_{\rm geom}(y), y) \sim A^{1/3} e^{-4\sqrt{\bar{\alpha}_s \lambda}\, y}. \tag{45}$$

That is, the nuclear modification factor is getting progressively suppressed in the forward direction. This suppression is much stronger than that in inclusive gluon production.

Approximately we can write

$$R^{pA}_{\rm diff}(k_T, y) \sim A^{1/3}\left(R^{pA}_{\rm incl}(k_T, y)\right)^2, \quad Q_s < k_T < Q_{\rm geom}. \tag{46}$$

Equation (46) clearly exhibits the higher twist nature of the diffractive gluon production. The peculiar properties of diffractive cross sections due to the higher twist contributions in nuclear and hadronic DIS have been discussed in Refs. [27] and [28].

3. *Saturation region*

In the saturation region we utilize Eq. (33) and one of either Eq. (24) or Eq. (25) in Eq. (31) and arrive at a rather involved expression. Keeping only the parametric dependence and omitting the logarithmic factors, we obtain

$$R^{pA}_{\rm diff}(R, k_T, y) \sim \frac{1}{A^{1/3}} \frac{k_T^4}{R^2\Lambda^4 Q_s^2}\, e^{2\sqrt{2\bar{\alpha}_s(Y-y)\ln(RQ_s)}} \times e^{-2\sqrt{2\bar{\alpha}_s(Y-y)\ln(Rk_T)}} e^{-4\sqrt{2\bar{\alpha}_s y \ln\frac{k_T}{\Lambda}}}, \quad k_T, \frac{1}{R} < Q_s. \tag{47}$$

There is a very strong suppression of diffractive gluon production in the saturation region in the case of low-x evolution. This suppression, however, is still milder than that in the quasiclassical case (38). On the critical line $k_T = Q_s(y)$ we get for forward rapidities ($Y - y \ll y$) and central collisions [employing Eq. (28)]

$$R^{pA}_{\rm diff}(Q_s(y), y) \sim e^{-4\sqrt{\bar{\alpha}_s\lambda}\, y}, \tag{48}$$

which implies a strong suppression in the forward direction.

IV. NUMERICAL CALCULATIONS

All the features that we discussed in the previous section can be visualized using a simple model for the forward elastic dipole–nucleus scattering amplitude $N_A(\mathbf{r}, \mathbf{b}, y)$. We parametrize it as [13]

$$N_A(\mathbf{r}, \mathbf{b}, y) = 1 - \exp\left\{-\tfrac{1}{4}\left(r^2 Q_s^2\right)^{\gamma(r,y)}\right\}. \tag{49}$$

The anomalous dimension is parametrized in such a way that it satisfies the analytically well-known limits of (i) $r \to 0$, y fixed and (ii) $y \to \infty$, r fixed:

$$\gamma(r, y) = \begin{cases} \frac{1}{2}\left(1 + \frac{\xi(r,y)}{|\xi(r,y)|+\sqrt{2|\xi(r,y)|+28\zeta(3)}}\right) & y \geqslant y_0, \\ 1 & y < y_0, \end{cases} \tag{50}$$

where

$$\xi(r, y) = \frac{\ln\left[1/\left(r^2 Q_{s0}^2\right)\right]}{(\lambda/2)(y - y_0)}. \tag{51}$$

In the double logarithmic approximation we can replace $r^2 \approx 1/(4k_T^2)$. The gluon saturation scale is given by

$$Q_s^2(y) = \Lambda^2 A^{1/3} e^{\lambda y} \left(\frac{\sqrt{s}}{200\,\text{GeV}}\right)^{\lambda}, \tag{52}$$

where parameters $\Lambda = 0.6$ GeV and $\lambda = 0.3$ are fixed by DIS data [29]. The initial saturation scale used in Eq. (51) is defined by $Q_{s0}^2 = Q_s^2(y_0)$, with y_0 the value of rapidity at which the small-x quantum evolution effects set in. Fit to the RHIC data yields $y_0 = 0.5$ [13].

Numerical calculations of the cross section (15) are performed after substitution of Eq. (21) with Eq. (49) and the following formula for the dipole density in diffusion approximation [cp. Eq. (29)]:

$$n_p(r, r', Y - y) = \frac{1}{2\pi^2}\frac{1}{rr'}\sqrt{\frac{\pi}{14\zeta(3)\bar{\alpha}_s\, d(Y-y)}} \times e^{(\alpha_P - 1)(Y-y)} e^{-\frac{\ln^2\frac{r}{r'}}{14\zeta(3)\bar{\alpha}_s d(Y-y)}}. \tag{53}$$

Parameter d is equal to unity in the LO BFKL. To obtain the hadron diffractive cross section we convoluted the obtained result with the LO pion fragmentation function given in Ref. [30]. Diffractive gluon production in pp collisions, which is required as a baseline for the calculation of the nuclear modification factor (31), is obtained by setting $A = 1$ in the formula for the corresponding cross section in pA collisions.

The results of numerical calculations are exhibited in Figs. 3–6. In Fig. 3 one can see that at RHIC $R^{pA} \sim 2 - 2.5$ at $y \simeq 0$ and $k_T > 2$ GeV. This enhancement is a signature

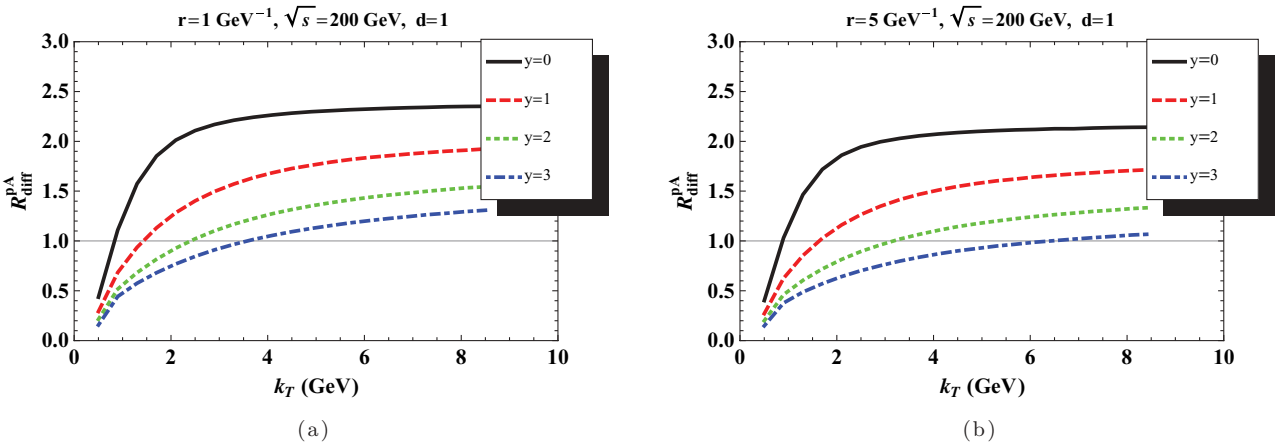

FIG. 3. (Color online) Nuclear modification factor for diffractive pion production in pA collisions at RHIC as a function of transverse momentum for two characteristic sizes of protons: (a) 0.2 fm and (b) 1 fm. The effects of finite coherence length are neglected.

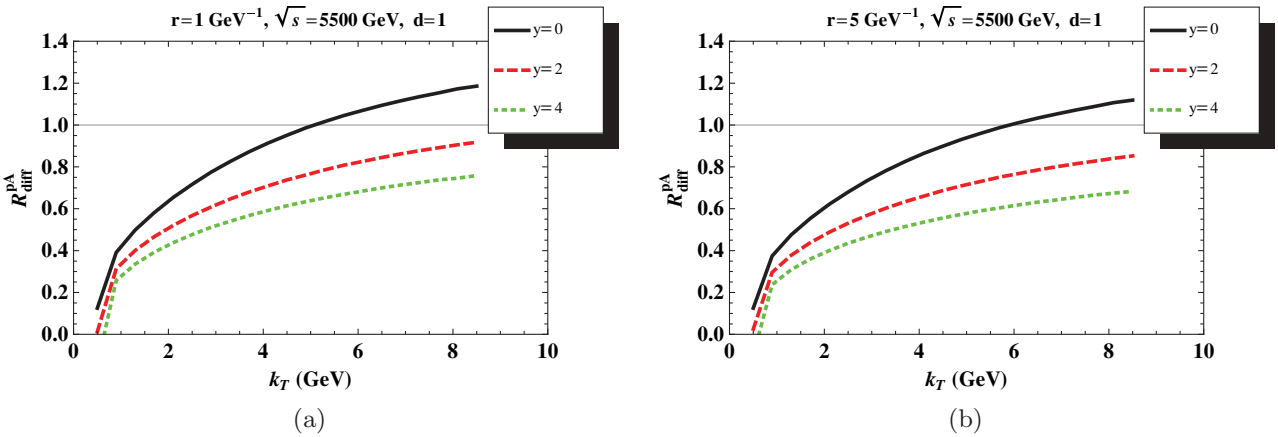

FIG. 4. (Color online) Nuclear modification factor for diffractive pion production in pA collisions at LHC as a function of transverse momentum for two characteristic sizes of protons: (a) 0.2 fm and (b) 1 fm. The effects of finite coherence length are neglected.

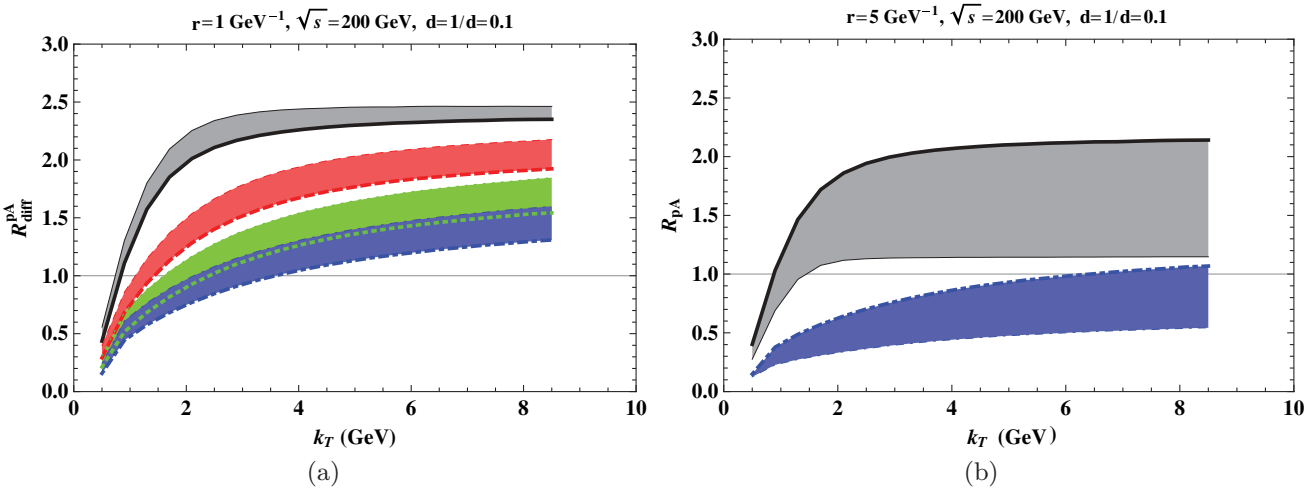

FIG. 5. (Color online) Effect of diffusion in the dipole sizes on the diffractive pion production at RHIC for two characteristic sizes of protons: (a) 0.2 fm and (b) 1 fm. The upper line of the same type corresponds to $d = 1$; the lower one corresponds to $d = 0.1$. Lines of different types correspond to different rapidities (notations are the same as those in Fig. 3). The effects of finite coherence length are neglected.

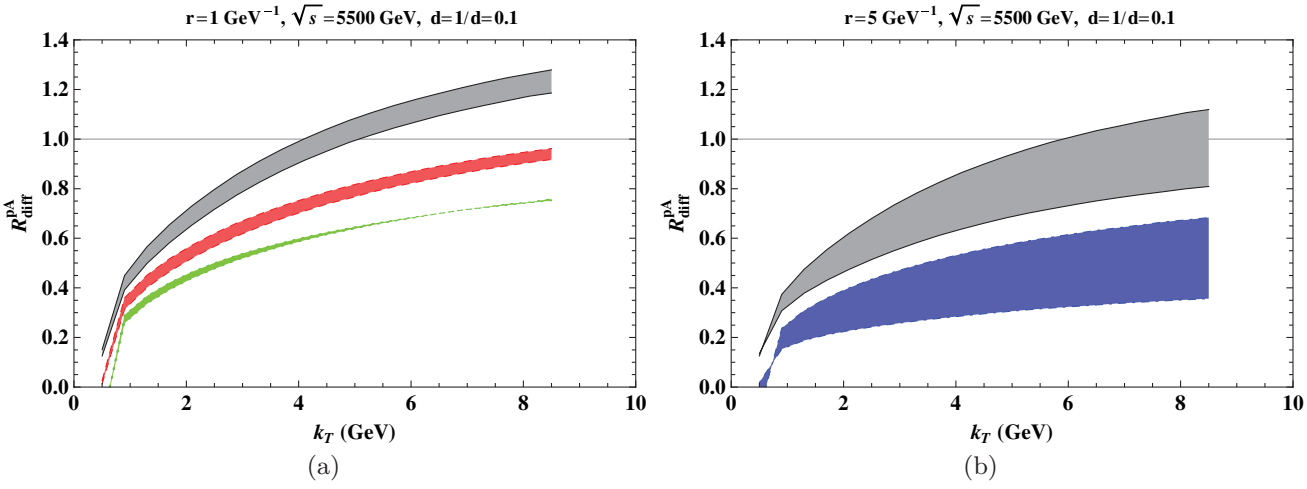

FIG. 6. (Color online) Effect of diffusion in the dipole sizes on the diffractive pion production at LHC for two characteristic sizes of protons: (a) 0.2 fm and (b) 1 fm. The upper line of the same type corresponds to $d = 1$; the lower one corresponds to $d = 0.1$. Lines of different types correspond to different rapidities (notations are the same as those in Fig. 4). The effects of finite coherence length are neglected.

of a leading power correction [see Eq. (43)]. As rapidity increases there are two important effects that take place in the proton and nucleus wave functions: (i) the spectrum of intermediate dipoles in a projectile proton shrinks as the rapidity interval available for the low-x evolution in proton becomes narrower; (ii) as y increases, x of gluon decreases causing stronger gluon saturation effect in the nucleus. Both effects lead to suppression of the nuclear modification factor. Gluon saturation in protons leads to the suppression law (45). Of course, the effect of diffusion in a proton is more pronounced for a proton with larger characteristic size, because in the absence of the evolution effects (i.e., in the quasiclassical approximation) the cross section would be exponentially suppressed [see Eq. (38)].

We further investigated the effect of diffusion by introducing the parameter d in Eq. (53). As has been repeatedly pointed out in this article, it is the BFKL diffusion that makes the diffractive gluon production possible by generating intermediate dipoles of small size. Gluon saturation effects in proton may tame the BFKL diffusion [31] leading to smaller effective diffusion coefficient. This effect is taken into account in Fig. 5 for RHIC and in Fig. 6 for LHC. The shadow region in all figures demonstrates the difference in the nuclear modification factor between the cases of $d = 1$ and $d = 0.1$. Switching off the diffusion severely impacts the nuclear modification factor at low energies/rapidities and for larger distances between the valence quarks in proton.

Unlike the nuclear modification factor for inclusive hadron production, which decreases as a function of rapidity and centrality at RHIC and reaches almost maximal possible suppression so that no significant additional suppression is expected at LHC, the diffractive hadron production shows a very interesting behavior even at LHC. This makes this process suitable for exploration of different kinematic regions at the high energy frontier. We believe that it will be instrumental in unraveling the structure and dynamics of strong gluon fields.

ACKNOWLEDGMENTS

We thank Dima Kharzeev, Yuri Kovchegov, and J.-W. Qiu for many informative discussions. The work of K.T. was supported in part by the U.S. Department of Energy under Grant DE-FG02-87ER40371. He would like to thank RIKEN, BNL, and the U.S. Department of Energy (Contract DE-AC02-98CH10886) for providing facilities essential for the completion of this work.

[1] L. V. Gribov, E. M. Levin, and M. G. Ryskin, Phys. Rep. **100**, 1 (1983).
[2] A. H. Mueller and J. W. Qiu, Nucl. Phys. **B268**, 427 (1986).
[3] L. McLerran and R. Venugopalan, Phys. Rev. D **49**, 2233 (1994); Phys. Rev. D **49**, 3352 (1994); Phys. Rev. D **50**, 2225 (1994).
[4] J. Jalilian-Marian, A. Kovner, and H. Weigert, Phys. Rev. D **59**, 014015 (1998).
[5] A. Kovner, J. G. Milhano, and H. Weigert, Phys. Rev. D **62**, 114005 (2000); H. Weigert, Nucl. Phys. **A703**, 823 (2002).
[6] E. Iancu and L. D. McLerran, Phys. Lett. **B510**, 145 (2001).
[7] Y. Li and K. Tuchin, Phys. Rev. D **77**, 114012 (2008).
[8] Y. Li and K. Tuchin, Nucl. Phys. A **807**, 190 (2008).
[9] E. Avsar, G. Gustafson, and L. Lonnblad, J. High Energy Phys. 07 (2005) 062.
[10] E. Avsar, G. Gustafson, and L. Lonnblad, J. High Energy Phys. 01 (2007) 012.
[11] E. Avsar, G. Gustafson, and L. Lonnblad, J. High Energy Phys. 12 (2007) 012.
[12] B. Z. Kopeliovich, I. K. Potashnikova, and I. Schmidt, Phys. Rev. C **73**, 034901 (2006).
[13] D. Kharzeev, Y. V. Kovchegov, and K. Tuchin, Phys. Lett. **B599**, 23 (2004).
[14] K. Tuchin, Nucl. Phys. **A798**, 61 (2008).
[15] Y. V. Kovchegov, Phys. Rev. D **64**, 114016 (2001); **68**(E), 039901 (2003).
[16] A. B. Kaidalov, V. A. Khoze, A. D. Martin, and M. G. Ryskin, Acta Phys. Pol. B **34**, 3163 (2003).
[17] E. Levin and K. Tuchin, Nucl. Phys. **B573**, 833 (2000).
[18] A. H. Mueller, Nucl. Phys. **B415**, 373 (1994); A. H. Mueller and B. Patel, *ibid.* **B425**, 471 (1994); A. H. Mueller, *ibid.* **B437**, 107 (1995).
[19] E. A. Kuraev, L. N. Lipatov, and V. S. Fadin, Sov. Phys. JETP **45**, 199 (1977) [Zh. Eksp. Teor. Fiz. **72**, 377 (1977)].
[20] I. I. Balitsky and L. N. Lipatov, Sov. J. Nucl. Phys. **28**, 822 (1978) [Yad. Fiz. **28** 1597 (1978)].
[21] I. Balitsky, Nucl. Phys. **B463**, 99 (1996).
[22] Y. V. Kovchegov, Phys. Rev. D **60**, 034008 (1999).
[23] A. H. Mueller, Nucl. Phys. **B335**, 115 (1990).
[24] D. Kharzeev, Y. V. Kovchegov, and K. Tuchin, Phys. Rev. D **68**, 094013 (2003).
[25] D. Kharzeev and K. Tuchin, Nucl. Phys. **A770**, 40 (2006).
[26] Y. Li and K. Tuchin, Phys. Rev. D **75**, 074022 (2007).
[27] E. Gotsman, E. Levin, U. Maor, L. D. McLerran, and K. Tuchin, Phys. Lett. **B506**, 289 (2001).
[28] E. Gotsman, E. Levin, U. Maor, L. D. McLerran, and K. Tuchin, Nucl. Phys. **A683**, 383 (2001).
[29] K. Golec-Biernat and M. Wusthoff, Phys. Rev. D **59**, 014017 (1999).
[30] B. A. Kniehl, G. Kramer, and B. Potter, Nucl. Phys. **B597**, 337 (2001).
[31] A. H. Mueller and D. N. Triantafyllopoulos, Nucl. Phys. **B640**, 331 (2002).